

The Conformational Distributions and Interconversions of Partially Methylated Calix[4]arenes

Willem P. van Hoorn, Martijn G. H. Morshuis, Frank C. J. M. van Veggel,* and David N. Reinhoudt*

Laboratory of SupraMolecular Chemistry and Technology, University of Twente, P.O. Box 217, 7500 AE Enschede, The Netherlands

Received: September 24, 1997; In Final Form: November 21, 1997

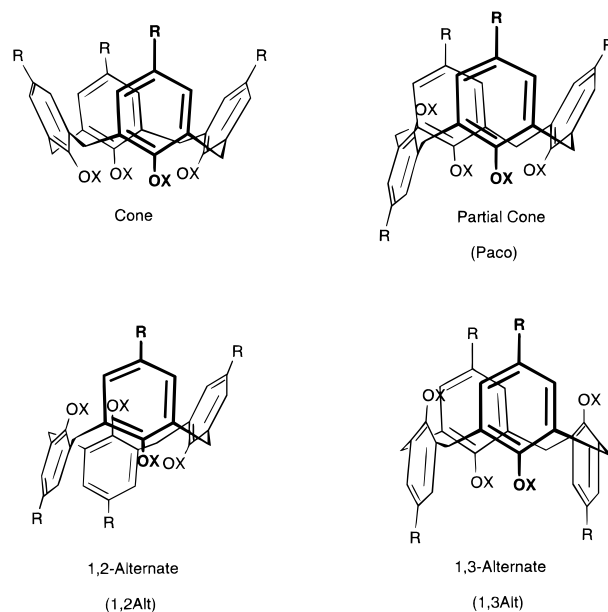
The conformational distributions and Cone \rightarrow Inverted Cone (Cone') interconversions of monomethoxy-, 1,2-dimethoxy-, 1,3-dimethoxy-, and trimethoxycalix[4]arenes **3a–6a** were investigated by molecular modeling. The calculated conformational distributions are generally in accordance with NMR data obtained for the *p*-*tert*-butyl derivatives **3b–6b**. Careful examination of all possible inversion pathways showed that the high inversion barriers of Cone \rightarrow Cone' interconversion are caused by the cooperative barriers of hydrogen bonds rupture and the steric barrier of rotating a methoxy group through the annulus. This cooperative effect is so strong that the Cone \rightarrow Cone' conversion is blocked at room temperature. The order of the calculated barriers for the Cone \rightarrow Inverted Cone interconversions is monomethoxy- (35.1 kcal mol⁻¹) > 1,2-dimethoxy- (32.2 kcal mol⁻¹) \approx 1,3-dimethoxy- (30.3 kcal mol⁻¹) > trimethoxycalix[4]arene (27.0 kcal mol⁻¹), values that are in good agreement with the available qualitative experimental results. The rate-limiting step involved in all cases is the rotation of a methoxy-bearing ring.

Introduction

Calix[*n*]arenes are cyclic oligomeric condensates of phenols and formaldehyde.¹ When *p*-*tert*-butylphenol is used, *p*-*tert*-butylcalix[4]arene **1b** can be isolated in a one-pot synthesis in high yield. The *tert*-butyl groups can easily be removed, yielding a molecule with eight selectively functionalizable positions in only two reaction steps. The convenient synthesis and control over the desired conformation² have made calix[4]arenes an extremely useful building block in supramolecular chemistry.¹ Calix[4]arenes can exist in four extreme conformations (Chart 1), designated the Cone, the Partial Cone (Paco), the 1,2-alternate (1,2Alt), and the 1,3-alternate (1,3Alt). The conformation of calix[4]arenes is not fixed at room temperature when the lower rim substituents are as small as OH or OMe.^{3–5} Substituents larger than OMe cannot pass through the annulus (at room temperature).^{6,7} By introducing sufficiently large lower rim substituents and by varying the reaction conditions, calix[4]arenes in the desired kinetically stable conformation can be obtained.² The partially methylated calix[4]arenes **3–6** are the intermediate structures between the tetramethoxycalix[4]arenes **2** and the tetrahydroxycalix[4]arenes **1**. Because the tetrahydroxy- and tetramethoxycalix[4]arenes are both conformationally flexible at room temperature, it was expected that the partially methylated calix[4]arenes **3–6** are conformationally flexible as well. However, it was argued by Gutsche et al.⁸ that both hydrogen bonding and steric interference reduce conformational mobility, the two effects combining to reach a maximum for the 1,2- and 1,3-dimethyl ethers. Recently, all possible partially methylated *p*-*tert*-butylcalix[4]arenes **3b–6b** (Chart 2) have been synthesized and studied by nuclear magnetic resonance (NMR) spectroscopy.^{4,9,10} The results for the partially methylated calix[4]arenes are summarized as follows:

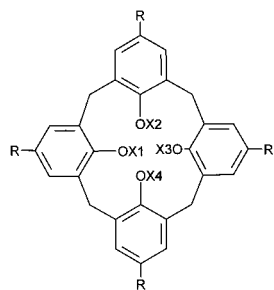
- The monomethoxy derivative **3b** exists in the cone conformation in CDCl₃, CCl₄, and CS₂ solutions.^{9,10} The NMR spectra

CHART 1: Four Extreme Conformations of Calix[4]arenes



recorded at higher temperatures (up to 125 °C in CDCl₂CDCl₂) did not show any change in the NMR spectrum. The cone \rightarrow cone' interconversion is completely blocked.

- The 1,2-dimethyl ether **4b** is present in CDCl₃ as a mixture of Cone (75%) and Paco (25%).¹⁰ The Paco is a mixture of two equivalent conformations in which the two rings bearing a methoxy group are anti to each other. These two Paco conformations interconvert rapidly at room temperature. At higher temperatures (105 °C), broadening of the signals was observed, which was interpreted as an indication that Cone \rightarrow Paco interconversion started to take place. However, the

CHART 2: Partially Methylated *p*-tert-Butylcalix[4]arenes 3b–6b

	OX1	OX2	OX3	OX4	R
1a	OH	OH	OH	OH	H
1b	OH	OH	OH	OH	<i>t</i> -Bu
2	OMe	OMe	OMe	OMe	
3a	OMe	OH	OH	OH	H
3b	OMe	OH	OH	OH	<i>t</i> -Bu
4a	OMe	OMe	OH	OH	H
4b	OMe	OMe	OH	OH	<i>t</i> -Bu
5a	OMe	OH	OMe	OH	H
5b	OMe	OH	OMe	OH	<i>t</i> -Bu
6a	OMe	OMe	OMe	OH	H
6b	OMe	OMe	OMe	OH	<i>t</i> -Bu

Cone \rightarrow Cone' interconversion was not observed. This result means that the energy barrier for rotation of the two phenol rings is low, but for the two anisole rings the barrier is high.¹¹

•The 1,3-dimethyl ether **5b** adopts a Cone conformation both in solution^{9,10} and in the solid state,¹² and does not show any sign of coalescence in the NMR spectrum at temperatures up to 125 °C in CDCl₂CDCl₂.

•The trimethoxycalix[4]arene **6b** crystallizes in the Cone conformation.¹² In the NMR spectrum in CDCl₃, the main conformation is the Cone,⁹ but other unidentified minor conformations are present as well.¹⁰ Full coalescence of the Cone signals has nearly been reached at 125 °C, indicating that this derivative is the most flexible of all partially methylated calix[4]arenes.

Surprisingly, the conformations of the partially methylated calix[4]arenes **3b–6b** are far less mobile than either the tetrahydroxy- or the tetramethoxycalix[4]arenes **1** and **2**, respectively. In fact, the Cone \rightarrow Cone' interconversion observed for tetrahydroxycalix[4]arenes is blocked for all partially methylated calix[4]arenes (at least up till 125 °C). We have earlier shown by molecular modeling that the inversion barrier of the tetrahydroxycalix[4]arenes **1** is due to the breaking of hydrogen bonds, and that the barriers of conformational interconversion the tetramethoxycalix[4]arenes **2** are due to steric repulsion of pushing a methoxy group through the annulus.¹³ The partially methylated calix[4]arenes contain both hydroxyl and methoxy moieties, and both types of barriers are assumed to be present. The low conformational mobility of the partially methylated calix[4]arenes indicates that both of these barriers show a cooperative effect that makes the combined barrier higher than that of each of the constituent barriers alone. We propose the following mechanism to explain this cooperative effect: For every conformation of calix[4]arenes having hydroxyl groups, the smallest diameter of the annulus is formed by these hydroxyl groups. This effect can most clearly be seen for the Cone of tetrahydroxycalix[4]arene **1a** (Figure 1), but also in other conformations of other calix[4]arenes.^{14,15} When a methoxy group swings through the annulus, the maximum steric barrier is encountered at the smallest diameter. The hydroxyl moieties forming hydrogen bonds have to make place for the methoxy group. This will elongate the OH \cdots O distances and weaken or break the hydrogen bonds. The hydroxyl group is too small to exert this "pushing aside" of the other hydroxyl moieties.¹³ Assuming this mechanism, the rate-limiting step in the conformational interconversion pathway will be the inversion of an aromatic ring bearing a methoxy moiety.

Monomethoxycalix[4]arenes **3** contain potentially the highest number of hydrogen bonds (3) of all partially methylated calix[4]arenes; so, for these derivatives, the cooperative effect will

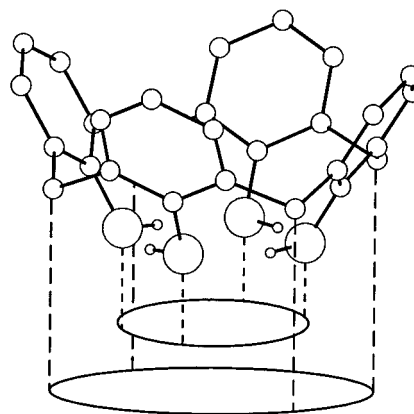


Figure 1. The energy-minimized Cone of tetrahydroxycalix[4]arene **1**. The smallest diameter of the annulus is found at the hydroxy moieties.

be strongest and the highest Cone \rightarrow Cone' energy barrier is expected. Dimethoxycalix[4]arenes **4** and **5** can both form two hydrogen bonds, and trimethoxycalix[4]arenes **6** can form only one. We predict therefore the following order in the inversion barriers: monomethoxy (highest) > 1,2-dimethoxy \approx 1,3-dimethoxy > trimethoxy (lowest). Gutsche *et al.*⁸ used similar reasoning but arrived at a different conclusion. They predicted that the cooperative effect is strongest in the 1,2- and 1,3-dimethyl derivatives. The prediction of Gutsche *et al.*⁸ is unlikely because only one methoxy group can pass through the annulus at a time, and the maximum steric barrier is already reached with one methyl group.

In this paper, reaction path calculations with the Conjugate Peak Refinement algorithm are used to investigate the inversion pathways of the partially methylated calix[4]arenes **3a–6a**. These derivatives were chosen instead of the *p*-tert-butyl derivatives to make computations faster. The calculations are analyzed with the following questions/hypotheses in mind:

•In which derivative is the combination of breaking the hydrogen bonds and steric repulsion the strongest cooperative effect? Our prediction is the monomethoxycalix[4]arene, whereas the prediction of Gutsche *et al.*⁸ is the 1,2- or 1,3-dimethoxycalix[4]arene.

•The rate-limiting step in the Cone \rightarrow Cone' inversion is an anisole ring flip because the methoxy moiety has to pass through the annulus to exert its steric influence.

Methods

Energy Minimization. Version 23f3 of the charmm¹⁶ program was used. Energies of the calix[4]arenes were evaluated with the parameters, partial charges, and energy function described in Fischer *et al.*¹³ The energies of the conformations were minimized until the root-mean-square value of the energy gradient was $<10^{-12}$ kcal mol⁻¹ Å⁻¹.

Normal Mode Calculation. All $3N$ (in which N the number of atoms) modes were calculated. Each energy-minimized conformation was checked to be a true minimum by checking the absence of negative frequencies and the presence of six zero frequencies. The maximum deviation from zero was in the order of ≈ 0.2 cm⁻¹. The classical (ΔA_{cl}) and quantum mechanical (ΔA_{qm}) vibrational free energies as well as the zero point correction energy (ΔA_0) were calculated¹⁷ with eqs 1–3:

$$\Delta A_{\text{QM}} = kT \sum_{i=7}^{3N} \ln(1 - e^{-h\nu_i/kT}) \quad (1)$$

$$\Delta A_{\text{cl}} = kT \sum_{i=7}^{3N} \ln\left(\frac{h\nu_i}{kT}\right) \quad (2)$$

$$\Delta A_0 = \sum_{i=7}^N \frac{h\nu_i}{2} \quad (3)$$

where k is the Boltzmann constant, T is the temperature in Kelvin, N is the number of atoms, h is the constant of Planck, and ν_i is the frequency of the i^{th} mode.

Calculation of Rotational Free Energy. The rotational free energy ΔA_{rot} was calculated¹⁸ with equation 4. Only the influence of the rotational symmetry number σ was taken into account, because earlier calculations with similar calix[4]arenes have shown that the product of the three moments of inertia was nearly constant and without influence on the calculated rotational free energy¹⁹:

$$\Delta A_{\text{rot}} \approx -kT \ln\{\pi^{1/2} T^{3/2} \sigma^{-1}\} \quad (4)$$

Boltzmann Distribution. The probability p of finding a conformation i is given by equation 5:

$$p(i) = \frac{n_i e^{-\Delta A_i/kT}}{\sum_{\text{all } i} n_i e^{-\Delta A_i/kT}} \times 100\% \quad (5)$$

$$\Delta A_i^{\text{QM}} = E_{\text{min}} + \Delta A_{\text{QM}} + \Delta A_0 + \Delta A_{\text{rot}}$$

$$\Delta A_i^{\text{cl}} = E_{\text{min}} + \Delta A_{\text{cl}} + \Delta A_{\text{rot}} \quad (6)$$

In these equations, n_i is the degeneracy of conformation i , and E_{min} is the minimized potential energy of i .

Conformational Degeneracy. The degeneracy n in Tables 3S–10S (Supporting Information) is determined by taking into account the skeleton of the calix[4]arene, the position(s) of the methoxy group(s), and the directionality of the OH moieties. The skeleton has the following degeneracy numbers: Cone 2 (0000, 1111), Paco 8 (1000, 0100, 0010, 0001, 01111, 1011, 1101, 1110), 1,2Alt 4 (1100, 0110, 0011, 1001), and 1,3Alt 2 (1010, 0101). The digits in the names of the conformations indicate which aromatic ring is inverted. The names of conformations are explained in more detail in the caption of Table 1. A methoxy moiety can be attached to one of the four aromatic rings. If all of these four rings are equivalent, the degeneracy is increased by a factor of 4. The directionality of the hydrogen bonds can either be clockwise or counterclockwise, which adds maximally a factor of 2 to the degeneracy. This method can be explained with two examples, the degeneracy is 16 for both 1000~A and 0001~A conformations of monomethoxycalix[4]arene **3a** in Figure 2. The 1000~A conformation is a Paco with the methoxy group attached to the inverted ring. The degeneracy of the Paco skeleton is 8. The position of the methoxy group is unique; there is only one way to attach a methoxy group to the inverted ring. The directionality of the hydrogen bonds is not unique; both conformations with a clockwise and counterclockwise H-bond directionality are equivalent. The degeneracy is, hence, 16: 8 (Paco) \times 1 (methoxy) \times 2 (hydrogen bonds). The 0001~A conformation

is a Paco with a methoxy group attached to an aromatic ring proximal to the inverted ring. To build this conformation, the methyl group can be attached to one of the two shaded oxygen atoms, yielding the 0001~A and 0100~A conformations. However, the clockwise and counterclockwise H-bond directions are not equivalent. The degeneracy becomes 16: 8 (Paco) \times 2 (methoxy) \times 1 (hydrogen bonds). All conformations in this paper have the same directionality of the hydrogen bonds; we used the fact that 0100~A (counterclockwise) = 0001~A (clockwise) to obtain the conformations with the counterclockwise hydrogen bond directionality. All inverted conformations and transition states have their noninverted equivalents; for instance 0001~A (clockwise) = 1110~B (counterclockwise).

Travel. The Conjugate Peak Refinement (CPR) algorithm^{20–22} searches for maxima along the adiabatic energy valley connecting two local minima on an adiabatic energy surface. These maxima are refined to saddle points and represent the transition states of the reaction pathway between the two minima. All the degrees of freedom of the molecule can contribute to the reaction path. There is no need to choose a reduced reaction coordinate, such as a rotation, around a certain bond. The algorithm has been integrated into charmm¹⁶ in the travel module.

Finding the Global Lowest Energy Path. The global lowest energy path is the path connecting the Cone with the Cone' with the lowest energy barrier. All partially methylated calix[4]arenes are found (mainly) in the Cone with NMR spectroscopy,^{9,10} so the same stepwise connection scheme as used previously¹³ for tetrahydroxycalix[4]arene **1a** was applied (Figure 3). The energy barrier is calculated relative to the global energy minimum. The partially methylated calix[4]arenes have a lower symmetry relative to either the tetrahydroxy or tetramethoxycalix[4]arenes. This lower symmetry increases the number of distinguishable conformers and transition states connecting them. Furthermore, the mirror plane of the Cone \rightarrow Cone' interconversion of tetrahydroxycalix[4]arene¹³ is no longer present [i.e. the 1,2Alt/1,3Alt \rightarrow Paco' \rightarrow Cone' part of the connection scheme (Figure 3) is no longer the mirror image of the Cone \rightarrow Paco \rightarrow 1,2Alt/1,3Alt part²³], which results in a very large number of possible pathways connecting Cone with Cone'. In Figure 4, an example is given with 1600 different possible pathways. The large number of possible pathways makes it virtually impossible to find the lowest energy path by hand. Therefore, a computer program has been written²⁴ that searches all possible pathways for the path with the lowest energy barrier. During the search it is assumed that the steps involving the rotation of a methoxy moiety always have a lower free energy barrier than the steps involving an aromatic ring flip. The tree in Figure 4 is searched with a recursive algorithm. There are multiple pathways in Figure 4 with the same energy barrier. For instance, assuming that the rate-limiting step is the 1,2Alt1 \rightarrow Paco1' step, and the 1,2Alt1 reactant can be reached via Cone1 \rightarrow Cone1 \rightarrow Paco1 \rightarrow Paco1 \rightarrow 1,2Alt1 \rightarrow 1,2Alt1 or via Cone1 \rightarrow Cone2 \rightarrow Paco3 \rightarrow Paco4 \rightarrow 1,2Alt2 \rightarrow 1,2Alt1. The first possibility contains some trivial steps and is therefore shorter. The output of the search program is the shortest path of all the lowest barrier pathways. The trivial steps are introduced to make the programming of the search program easier.

Results and Discussion

Ground States. The results of the energy minimizations of **3a–6a** are presented in Tables 3S, 5S, 7S, and 9S, respectively (Supporting Information). A summary of these tables containing

TABLE 1: Selected Results of Energy Minimizations and Vibrational and Rotational Free Energy Calculations of All Conformations of Partially Methylated Calix[4]arenes 3a–6a at $T = 300\text{ K}$.^{a,b}

conformer ^c	E_{\min}	ΔA_{QM}	ΔA_{cl}	ΔA_0	σ	n	ΔA_{rot}	ΔA_{total}		Boltzmn%																																																																																																																																																																																																																																																																																																																																																																																					
								QM	cl	QM	cl																																																																																																																																																																																																																																																																																																																																																																																				
3a																																																																																																																																																																																																																																																																																																																																																																																															
0000~A	0.0	0.0	0.0	0.0	1	16	0.0	0.0	0.0	99.1	99.1																																																																																																																																																																																																																																																																																																																																																																																				
0000~A \Rightarrow	5.0	-0.2	-0.6	-0.6	1	8	0.0	4.5	4.8	0.1	0.0																																																																																																																																																																																																																																																																																																																																																																																				
1000~B	3.0	0.1	0.0	-0.1	1	16	0.0	3.0	3.0	0.6	0.6																																																																																																																																																																																																																																																																																																																																																																																				
1000~A	5.0	-0.6	-1.1	-0.7	1	16	0.0	3.7	3.9	0.2	0.1	0100~A	5.6	-0.6	-1.2	-0.9	1	16	0.0	4.1	4.4	0.1	0.1	4a												0000~AA	0.6	-0.6	-0.8	-0.5	1	16	0.0	0.0	0.0	53.7	48.7	0100~AB	0.0	0.0	0.0	0.0	1	16	0.0	0.4	0.2	27.9	35.2	0100~AA	1.9	-0.9	-1.3	-0.7	1	16	0.0	0.7	0.7	17.0	14.7	1000~BA	2.8	-0.6	-0.8	-0.3	1	16	0.0	2.3	2.2	1.2	1.3	1000~AA	5.1	-1.1	-1.7	-0.9	1	16	0.0	3.5	3.6	0.2	0.1	5a												0000~AA	0.0	0.0	0.0	0.0	2	8	0.0	0.0	0.0	96.1	96.5	0010~AB	3.0	0.1	0.2	0.1	1	8	-0.4	2.8	2.7	0.8	1.0	0001~AA	5.1	-0.6	-1.0	-0.7	1	8	-0.4	3.4	3.6	0.3	0.2	0010~AA	5.4	-0.4	-0.8	-0.5	1	16	-0.4	3.6	3.7	0.2	0.2	0010~AB \Rightarrow	3.6	0.3	0.3	0.0	1	8	-0.4	3.5	3.5	0.3	0.3	0010~AA \Rightarrow	5.3	-0.4	-0.8	-0.5	1	8	-0.4	4.0	4.1	0.1	0.1	0110~AA	4.2	-0.4	-0.5	-0.1	1	8	-0.4	3.3	3.3	0.4	0.4	6a												0000~AAA ^d	1.5	-0.2	-0.6	-0.5	1	16	0.0	0.7	0.9	12.1	9.9	0000~AAA ^d	1.9	-0.6	-1.0	-0.6	1	16	0.0	0.7	0.9	12.0	9.7	0100~ABA	0.0	0.0	0.0	0.0	1	16	0.0	0.0	0.0	40.7	47.5	0010~AAB	0.6	0.2	0.2	0.1	1	16	0.0	0.8	0.8	10.8	13.3	0100~AAA	1.9	-0.6	-1.0	-0.6	1	16	0.0	0.6	0.8	15.1	11.7	0100~AAB	2.0	0.7	0.9	0.3	1	16	0.0	2.9	2.9	0.3	0.4	0010~AAA	2.4	-0.6	-1.0	-0.6	1	16	0.0	1.2	1.4	5.6	4.6	1000~BAA	2.9	-0.3	-0.6	-0.3	1	16	0.0	2.2	2.3	1.0	1.1	0001~AAA	3.7	-0.5	-1.0	-0.9	1	16	0.0	2.4	2.7	0.8	0.5	0110~ABA	3.6	0.0	0.2	0.3	1	16	0.0	3.9	3.8	0.1	0.1	0110~AAB	3.8	-0.1	0.1	0.2	1	16	0.0	4.0	3.9	0.1	0.1	0110~AAA	5.1	-1.8	-2.3	-0.6	1	16	0.0	2.7	2.9	0.4	0.4	0101~BAA	3.6	-0.3	-0.6	-0.3	1	16	0.0	3.0	3.0	0.3	0.3	0101~AAB	4.1	-0.3	-0.6	-0.4	1	16	0.0	3.4	3.5	0.2	0.1	0101~AAA	4.2	-0.6	-1.2	-1.0	1	16	0.0	2.6	3.0	0.5	0.3
0100~A	5.6	-0.6	-1.2	-0.9	1	16	0.0	4.1	4.4	0.1	0.1																																																																																																																																																																																																																																																																																																																																																																																				
4a																																																																																																																																																																																																																																																																																																																																																																																															
0000~AA	0.6	-0.6	-0.8	-0.5	1	16	0.0	0.0	0.0	53.7	48.7																																																																																																																																																																																																																																																																																																																																																																																				
0100~AB	0.0	0.0	0.0	0.0	1	16	0.0	0.4	0.2	27.9	35.2																																																																																																																																																																																																																																																																																																																																																																																				
0100~AA	1.9	-0.9	-1.3	-0.7	1	16	0.0	0.7	0.7	17.0	14.7																																																																																																																																																																																																																																																																																																																																																																																				
1000~BA	2.8	-0.6	-0.8	-0.3	1	16	0.0	2.3	2.2	1.2	1.3																																																																																																																																																																																																																																																																																																																																																																																				
1000~AA	5.1	-1.1	-1.7	-0.9	1	16	0.0	3.5	3.6	0.2	0.1																																																																																																																																																																																																																																																																																																																																																																																				
5a																																																																																																																																																																																																																																																																																																																																																																																															
0000~AA	0.0	0.0	0.0	0.0	2	8	0.0	0.0	0.0	96.1	96.5																																																																																																																																																																																																																																																																																																																																																																																				
0010~AB	3.0	0.1	0.2	0.1	1	8	-0.4	2.8	2.7	0.8	1.0																																																																																																																																																																																																																																																																																																																																																																																				
0001~AA	5.1	-0.6	-1.0	-0.7	1	8	-0.4	3.4	3.6	0.3	0.2																																																																																																																																																																																																																																																																																																																																																																																				
0010~AA	5.4	-0.4	-0.8	-0.5	1	16	-0.4	3.6	3.7	0.2	0.2																																																																																																																																																																																																																																																																																																																																																																																				
0010~AB \Rightarrow	3.6	0.3	0.3	0.0	1	8	-0.4	3.5	3.5	0.3	0.3																																																																																																																																																																																																																																																																																																																																																																																				
0010~AA \Rightarrow	5.3	-0.4	-0.8	-0.5	1	8	-0.4	4.0	4.1	0.1	0.1																																																																																																																																																																																																																																																																																																																																																																																				
0110~AA	4.2	-0.4	-0.5	-0.1	1	8	-0.4	3.3	3.3	0.4	0.4																																																																																																																																																																																																																																																																																																																																																																																				
6a																																																																																																																																																																																																																																																																																																																																																																																															
0000~AAA ^d	1.5	-0.2	-0.6	-0.5	1	16	0.0	0.7	0.9	12.1	9.9																																																																																																																																																																																																																																																																																																																																																																																				
0000~AAA ^d	1.9	-0.6	-1.0	-0.6	1	16	0.0	0.7	0.9	12.0	9.7																																																																																																																																																																																																																																																																																																																																																																																				
0100~ABA	0.0	0.0	0.0	0.0	1	16	0.0	0.0	0.0	40.7	47.5																																																																																																																																																																																																																																																																																																																																																																																				
0010~AAB	0.6	0.2	0.2	0.1	1	16	0.0	0.8	0.8	10.8	13.3																																																																																																																																																																																																																																																																																																																																																																																				
0100~AAA	1.9	-0.6	-1.0	-0.6	1	16	0.0	0.6	0.8	15.1	11.7																																																																																																																																																																																																																																																																																																																																																																																				
0100~AAB	2.0	0.7	0.9	0.3	1	16	0.0	2.9	2.9	0.3	0.4																																																																																																																																																																																																																																																																																																																																																																																				
0010~AAA	2.4	-0.6	-1.0	-0.6	1	16	0.0	1.2	1.4	5.6	4.6																																																																																																																																																																																																																																																																																																																																																																																				
1000~BAA	2.9	-0.3	-0.6	-0.3	1	16	0.0	2.2	2.3	1.0	1.1																																																																																																																																																																																																																																																																																																																																																																																				
0001~AAA	3.7	-0.5	-1.0	-0.9	1	16	0.0	2.4	2.7	0.8	0.5																																																																																																																																																																																																																																																																																																																																																																																				
0110~ABA	3.6	0.0	0.2	0.3	1	16	0.0	3.9	3.8	0.1	0.1																																																																																																																																																																																																																																																																																																																																																																																				
0110~AAB	3.8	-0.1	0.1	0.2	1	16	0.0	4.0	3.9	0.1	0.1																																																																																																																																																																																																																																																																																																																																																																																				
0110~AAA	5.1	-1.8	-2.3	-0.6	1	16	0.0	2.7	2.9	0.4	0.4																																																																																																																																																																																																																																																																																																																																																																																				
0101~BAA	3.6	-0.3	-0.6	-0.3	1	16	0.0	3.0	3.0	0.3	0.3																																																																																																																																																																																																																																																																																																																																																																																				
0101~AAB	4.1	-0.3	-0.6	-0.4	1	16	0.0	3.4	3.5	0.2	0.1																																																																																																																																																																																																																																																																																																																																																																																				
0101~AAA	4.2	-0.6	-1.2	-1.0	1	16	0.0	2.6	3.0	0.5	0.3																																																																																																																																																																																																																																																																																																																																																																																				

^a Energies in kcal mol⁻¹ and relative to 0000~A, 0100~AA, 0000~AA, and 0100~ABA for **3a–6a**, respectively. ^b E_{\min} = minimized potential energy; ΔA_{QM} = quantum mechanical vibrational free energy; ΔA_{cl} = classical vibrational free energy; ΔA_0 = zero-point energy; σ = rotational symmetry number; n = degeneracy of conformation; ΔA_{rot} = rotational free energy; $\Delta A_{\text{total}} = E_{\min} + (\Delta A_{\text{QM}} + \Delta A_0 \text{ or } \Delta A_{\text{cl}}) + \Delta A_{\text{rot}} - kT \ln(n)$. ^c The digits in the names of the conformations indicate which aromatic ring is inverted. The letters indicate whether the methoxy group attached to each aromatic ring points outward (A) or inward (B). For example: 1000~B is a Paco in which the methoxy group on the inverted aromatic ring points inward. The methoxy group of monomethoxycalix[4]arene **3** is always attached to ring number 1, the two methoxy groups of 1,2-dimethoxycalix[4]arene **4** are always attached to rings 1 and 2, etc. A \Rightarrow sign indicates a conformation with one OH having counterclockwise directionality (instead of clockwise). ^d 0000~AAA with lowest minimized energy is the X-ray conformation (OH/OMe bearing rings bend outside, OMe/OMe bearing rings parallel to annulus). This conformation is opposite for the second 0000~AAA conformation.

all conformers of **3a–6a** with a calculated abundance of $\geq 0.1\%$ is presented in Table 1. In some conformations, reversal of the directionality of a hydrogen bond can yield low-energy conformations. These conformations have also been considered and are marked with \Rightarrow .

(i) *Monomethoxycalix[4]arene 3a*. The energy-minimized conformers of **3** are presented in Table 3S together with the vibrational and rotational free energy contributions. Two conformers have been added in which two hydroxyl hydrogens point at one methoxy oxygen, 0000~A \Rightarrow and 0010~A \Rightarrow , respectively (See Figure 5 for an example of a \Rightarrow conformation). These conformations do not significantly contribute to the Boltzmann distribution. Two hydrogen bonds pointing at one acceptor brings two positively charged hydrogens in close proximity, which is less favorable. The Cone of **3a** can be pinched in two ways: either the OH-bearing rings are parallel to each other and one methoxy-bearing ring and one OH-bearing ring are more perpendicular to the annulus, or the other way round. Both extremes were considered and they changed to the same nearly “perfect” Cone conformation upon energy

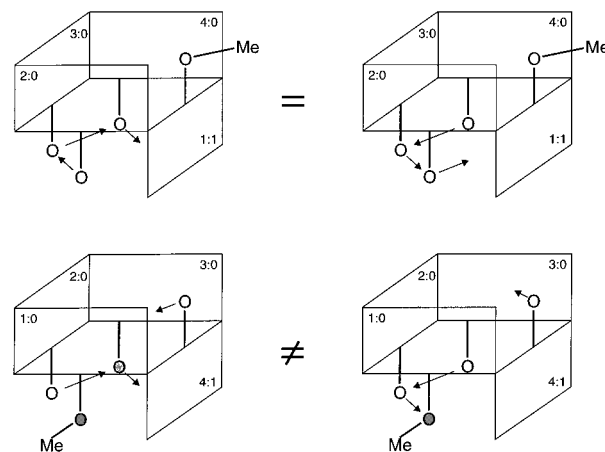


Figure 2. Schematic drawings of the 1000~A (upper) and 0001~A (lower) conformations of monomethoxycalix[4]arene **3a**. The arrows indicate O \rightarrow H bonds. Aromatic rings are numbered 1 to 4. The degeneracy of both conformations is 16 (see text).

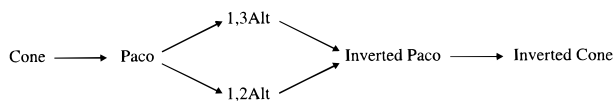


Figure 3. Example of a stepwise connection scheme for tetrahydroxycalix[4]arene **1a**.

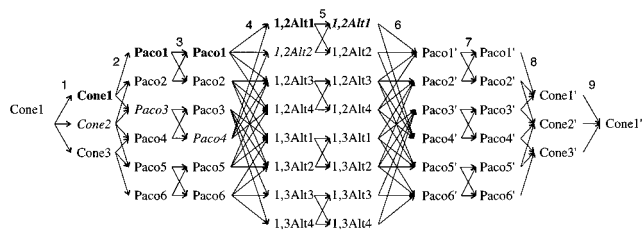


Figure 4. Example of all possible stepwise pathways connecting the Cone with the inverted Cone (Cone'). In steps 1, 3, 5, 7, and 9 methoxy groups can exchange inside and outside positions. Steps 2, 4, 6, and 8 are aromatic ring flips. In this example, the total number of pathways connecting Cone with Cone' is 1600. Two different pathways to reach **1,2Alt1** are indicated with bold or italic (see text). This example is not describing any one calix[4]arene in particular.

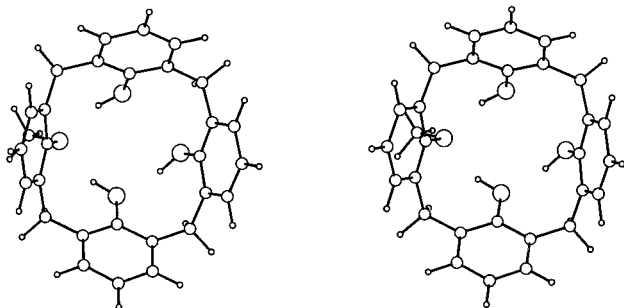


Figure 5. The 0000~A⇔ conformation of **3a**.

minimization.²⁵ The calculations predict the 0000~A Cone to be present in 99% abundance (i.e., a Cone with the methoxy group pointing outward; Figure 6a). This is in agreement with ¹H NMR spectroscopy of the *p*-*tert*-butyl derivative **3b** in CDCl₃, where the Cone was the only conformer found.^{9,10} The low field position of the methyl hydrogens (4.10 ppm)⁹ indicates that the methoxy group is not in the shielding zone of the aromatic rings, which is also in agreement with the calculations. The Cone conformation with the methoxy moiety pointing inward, 0000~B, has a significantly higher energy because the methoxy group hinders the hydrogen bonds and cannot act as a hydrogen-bond donor. The similarity of the NOE contacts between the methylene bridge hydrogens and the aromatic hydrogens of the monomethoxycalix[4]arene and tetrahydroxycalix[4]arene was interpreted by Alfieri *et al.*⁹ that both calix[4]arenes adopt a “perfect” Cone conformation in which all aromatic rings have the same angle with respect to the mean plane of the methylene bridges. This perfect Cone conformation is also found by calculations for the lowest energy conformer 0000~A. The calculated C^{para}—C^{para} distances between the opposite rings bearing hydroxyls is 8.6 Å and 7.8 Å between the opposite hydroxyl- and methoxy-bearing rings, respectively. For the Cone of tetrahydroxycalix[4]arene, both distances are 8.3 Å.¹³

(ii) *1,2-Dimethoxycalix[4]arene 4a*. The results of the ground-state calculations of **4a** are presented in Table 5S. Two conformations have been added in which the hydrogen bonds are not all pointing in the same direction, 0000~AA⇔ and 0110~AA⇔. Only the latter is stable, and 0000~AA⇔ changes to 0000~AA upon energy minimization (Figure 6b). The

calculated conformational distribution is 53.7% Cone and 46.2% Paco when the quantum mechanical vibrational contribution is included. The experimental Cone:Paco ratio of **4b** ranges from 4.3:1 (CS₂) to 1.2:1 (CCl₄).¹⁰ The best agreement between calculations in vacuo and experiment is expected for the latter, least polar solvent, and this agreement is indeed found. The Paco found by NMR has one of the two anisole rings flipped,¹⁰ which is also found by calculations (0100~AB and 0100~AA). The two 0100 conformations are stable because the two hydrogen bonds present in the 0000~AA Cone are also present in these conformations (Figure 6c–d). The methoxy moiety connected to the flipped aromatic ring of 0100~AB is pointing into the cavity. In the NMR spectrum, only one methoxy signal is found for the Paco at 2.94 ppm.¹⁰ This value is close to the methoxy signals of 1,2Alt (2.99 ppm) and 1,3Alt (2.87 ppm) of the *p*-*tert*-butyl-tetramethoxycalix[4]arene.⁵ For these conformations, we have postulated a fast exchange between inside and outside positions of the methoxy groups, which results in one average signal in NMR.¹³ The average signal is intermediate to the high-field signal of the inside position (≈2 ppm) and the low-field position of the outside position (≈4 ppm). Therefore, we interpret the methoxy signal found by NMR for the Paco of 1,2-dimethoxycalix[4]arenes **4** by a fast exchange of the 0100~AB and 0100~AA conformations. This interpretation is supported by the low free energy barrier (including ΔA[‡]_{QM}) calculated for the 0100~AB → 0100~AA interconversion (i.e., 7.8 kcal mol⁻¹).

(iii) *1,3-Dimethoxycalix[4]arene 5a*. This derivative has the highest number of possible symmetry elements, therefore the number of distinguishable conformers is relatively low. There are four possible conformations in which two hydroxyl moieties point toward one methoxy group (marked ⇔). These conformations do not significantly contribute to the calculated Boltzmann distribution (Table 7S). Like the Cone of monomethoxycalix[4]arene **3a**, the Cone conformation of **5a** can be pinched in two ways: either the OH-bearing rings are parallel to each other and the two methoxy-bearing rings more perpendicular to the annulus, or vice versa. The X-ray conformations of both **5a** and **5b** have the methoxy-bearing aromatic rings almost coplanar.¹² We also considered the Cone conformation with the two OH-bearing rings coplanar, but it changed to the X-ray conformation upon energy minimization (Figure 6e). The calculated conformational distribution shows almost exclusively Cone with traces of Paco and 1,2Alt. The calculated conformational distribution is in excellent agreement with the distribution of **5b** in CDCl₃ determined with NMR, where the Cone was found as the only conformer present.^{9,10} The lowest energy conformation 0000~AA is a Cone with both methoxy groups pointing outward, in accordance with the low field position of the methoxy protons (3.89 ppm) in the NMR spectrum in CDCl₃.⁹ Like the X-ray conformation, the NOE contacts measured indicate a “pinched” Cone in which the two anisole rings are almost coplanar, and the two phenol rings are more perpendicular to the annulus.⁹ The low stability of the Paco of the 1,3-dimethoxy derivative compared with the 1,2-dimethoxy derivative can be explained by looking at the positions of the methoxy moieties. The 1,3-positions do not allow for a Paco with two circular hydrogen bonds, as was the case for the 0100~AB and 0100~AA conformations of 1,2-dimethoxycalix[4]arene **4a**. A Paco with two hydrogen bonds is only possible for the 1,3-dimethoxy compound if the two hydroxyl moieties point toward the same methoxy group (i.e., the 0010~AB⇔ and 0010~AA⇔ conformations). This type of hydrogen bonding is less favorable than the circular type.

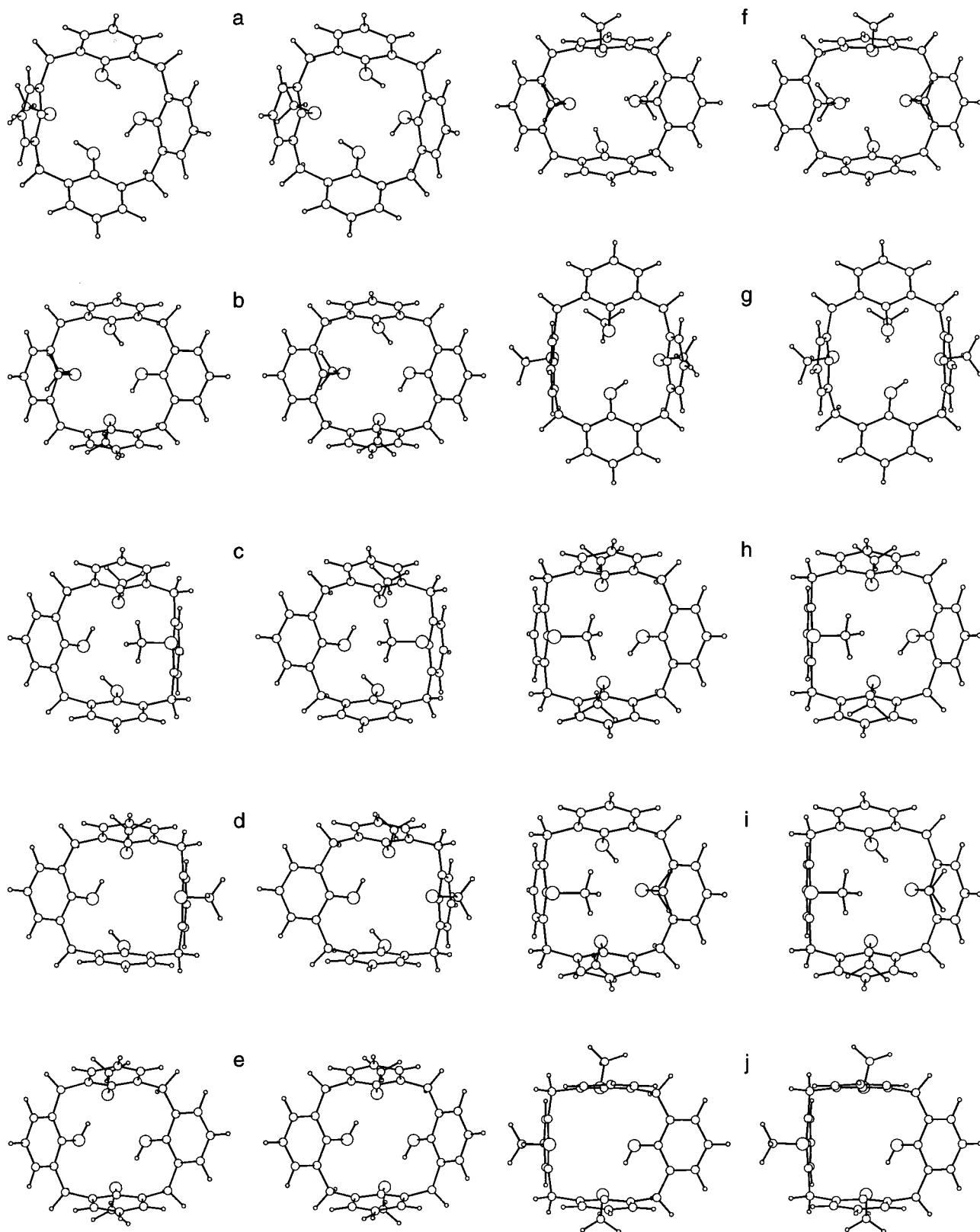


Figure 6. Energy-minimized conformations of the partially methylated calix[4]arenes **3a**–**6a**: **3a**: 0000~A (a); **4a**: 0000~AA (b); **4a**: 0100~AB (c); **4a**: 0100~AA (d); **5a**: 0000~AA (e); **6a**: 0000~AAA [f–g]; conformation (g) is built from the X-ray conformation of **6b**; the conformation (f) is the other stable pinched Cone conformer]; **6a**: 0100~ABA (h); **6a**: 0010~AAB (i); and **6a**: 0100~AAA (j).

(iv) *Trimethoxycalix[4]arene 6a*. Like the mono- and 1,3-dimethoxycalix[4]arenes **3a** and **5a**, the Cone can be pinched in two different ways (Figure 6f–g). For trimethoxycalix[4]arene **6a**, both 0000~AAA conformations are stable (Table 9S). The calculations predict the Paco to be the major conformer (79.1% classically, 74.4% quantum mechanically), whereas the

Cone is predicted to be present in 19.6% (classically) or 24.2% (quantum mechanically). NMR spectroscopy of *p*-*tert*-butyl derivative **6b** in CDCl₃ yields predominantly Cone with some minor unidentified conformer(s).^{9,10} The presence or absence of *p*-*tert*-butyl moieties can significantly influence the stability of the Cone of tetramethoxycalix[4]arenes **2**,²⁶ as can the

TABLE 2: Pathways and Free Energy Barriers (kcal mol⁻¹) for the Lowest Energy Cone → Cone' Interconversions of Partially Methylated Calix[4]arenes 3a–6a^{a,b}

compound	Cone → Paco	Paco → 1,2Alt/1,3Alt	1,2Alt/1,3Alt → Paco'	Paco' → Cone'
		Global optimal pathways:		
3a	0000~a	0001~a	0101 ~a	1101~a
	→ 13.1 →	→ 16.2 →	→ 35.1 →	→ 25.7 →
4a	0001~a	0101~a	1101 ~b	1111~a
	0000~ab	0001 ~ab	0101~aa	0111~aa
5a	→ 22.2 →	→ 32.2 →	→ 13.9 →	→ 29.2 →
	0001~ab	0101 ~aa	0111~aa	1111~ba
6a	0000~aa	0001~aa	0101~aa	0111 ~aa
	→ 9.3 →	→ 12.1 →	→ 28.7 →	→ 30.3 →
6a	0001~aa	0101~aa	0111~ab	1111 ~ba
	0000 ~aba	0100~aaa	0101~aaa	0111~aaa
6a	→ 27.0 →	→ 10.8 →	→ 26.7 →	→ 26.6 →
	0100 ~aaa	0101~aaa	0111~aab	1111~baa
		Pathways forced via the 1,2Alt:		
3a	0000~A	0001~A	0011~A	0111~A
	→ 13.1 →	→ 12.5 →	→ 10.3 →	→ 35.5 →
4a	0001~A	0011~A	0111~A	1111~B
	0000~AB	0100~AA	0110~AA	0111~AA
5a	→ 32.3 →	→ 7.6 →	→ 7.2 →	→ 29.2 →
	0100~AA	0110~AA	0111~AA	1111~BA
6a	0000~AB	0001~AB	0011~AA	0111~AA
	→ 12.0 →	→ 32.2 →	→ 6.3 →	→ 30.3 →
6a	0001~AB	0011~AA	0111~AA	1111~BA
	0000~AAB	0010~AAA	0011~AAA	1011~AAA
6a	→ 27.2 →	→ 7.5 →	→ 28.2 →	→ 27.0 →
	0010~AAA	0011~AAA	1011~BAA	1111~ABA

^a In/out rotations of methoxy groups are not shown. The rate-limiting step is shown in bold. The free energy barrier was calculated including ΔA_{QM} . ^b Abbreviations and names of conformations in the caption of Table 1.

solvent.^{10,27} The most stable Cone 0000~AAA is only 0.9 kcal mol⁻¹ (classically) or 0.7 kcal mol⁻¹ (quantum mechanically) higher in energy than the most stable Paco conformer 0100~ABA; hence, these effects need not to be large to make the Cone the most stable conformer. The unidentified minor conformers found by NMR^{9,10} are most probably the 0100~ABA, 0100~BAA, and 0100~AAA Paco conformers (Figures 6h–j). The presence of either 1,2Alt or 1,3Alt is predicted to be unlikely.

Interconversions. The calculated transition state energies of the calix[4]arenes **3a–6a** are presented in Tables 4S, 6S, 8S, and 10S, respectively (Supporting Information). For all calixarenes **3a–6a**, the lowest energy conversions are phenol ring flips, which have an upper limit of ≈ 20 kcal mol⁻¹, and the highest energy conversions are anisole ring flips, with a lower free energy limit of ≈ 25 kcal mol⁻¹. This energy gap between anisole and phenol ring flips is found for all partially methylated calixarenes in all interconversions. This gap confirms our hypothesis that the rate-limiting step for the Cone → Cone' interconversion is the rotation of a methoxy-bearing ring.

The optimal pathways for the Cone → Cone' interconversions have been determined by calculating all possible pathways (See *Methods*). The results are presented in Table 2 and Figure 7. The pathways of inversion shown were calculated with the free energy barriers containing the quantum mechanical vibrational contribution. With the classical contribution, exactly the same pathways were found. The order of the free energy barriers is monomethoxy (highest) > 1,2-dimethoxy \approx 1,3-dimethoxy > trimethoxy (lowest). This order agrees with our prediction that monomethoxycalix[4]arene **3a** should have the highest inversion barrier. All Cone → Cone' pathways proceed via a 1,3Alt intermediate. The Cone → Cone' interconversions have also been calculated without considering pathways via the 1,3Alt. (Table 2), yielding pathways via the 1,2Alt with only marginally higher free energy barriers. The lower steric barrier for the Paco/1,3Alt anisole ring rotations compared with the Paco→1,2Alt

pathways was also found for tetramethoxycalix[4]arenes **2**.¹³ The 1,3Alt conformers of calix[4]arenes have apparently the annulus with the smallest steric barrier for rotation of the lower rim substituent.

For the mono and 1,2-dimethoxy derivatives **3a** and **4a**, the rate-limiting steps are Paco→1,3Alt conversions, whereas for the 1,3-di- and trimethoxy derivatives **5a** and **6a**, the rate-limiting steps are Cone→Paco conversions. For **4a–6a**, the energy differences between the Paco→1,3Alt anisole rotations and the Cone→Paco anisole ring rotations is small, as can be seen in Table 2. For **3a**, the lowest Cone→Paco anisole ring rotation can be found in Table 4S (0000~B → 1000~A), and the difference in the free energy barrier is also small compared with the Paco→1,3Alt conversion (0.4 kcal mol⁻¹ higher). The strength of the hydrogen bonds in the Cone increases in the order mono- (strongest) > 1,2di- → 1,3di- → trimethoxycalix[4]arene (least strong).²⁸ In the 1,3Alt, all hydrogen bonds are broken, which apparently increases the free energy enough to make the Paco→1,3Alt steps rate limiting for **3a** and **4a**. The hydrogen bonds have less influence on the conformational free energy for **5a** and **6a**, the higher (steric) free energy barrier of the Cone→Paco over the Paco→1,3Alt conversions determines the position of the rate-limiting step.

The calculated free energy barriers for Cone→Cone' interconversion are all ≥ 27 kcal mol⁻¹. The reaction rate k_1 can be estimated with eq 7:

$$k_1 = \frac{kT}{h} \exp\left\{\frac{-\Delta A^\ddagger}{RT}\right\} \quad (7)$$

In this equation k is the Boltzmann constant, and h is Planck's constant. At $T = 300$ K, and with $\Delta A^\ddagger \geq 27$ kcal mol⁻¹, k_1 becomes $\leq 1.3 \times 10^{-7}$ s⁻¹. This result means that the Cone → Cone' interconversion is blocked at room temperature. This result is in agreement with NMR experiments.¹⁰ Other conformational interconversions are still possible, especially when

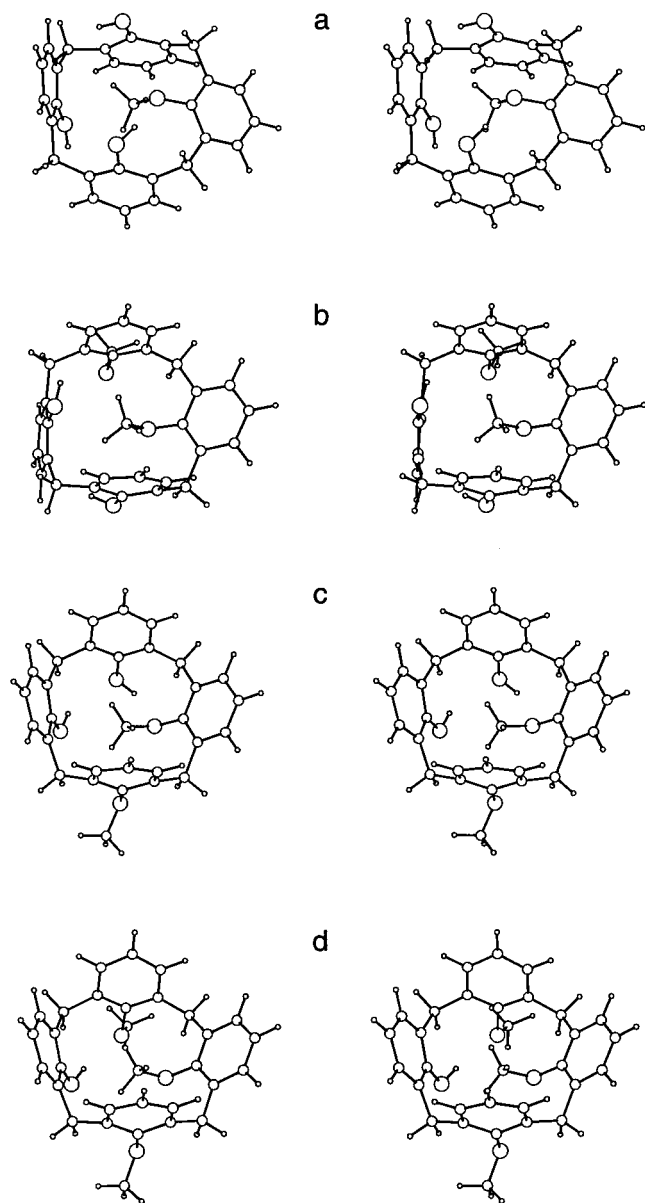


Figure 7. Rate-limiting transition states (See Table 2) for the Cone \rightarrow Cone' interconversions of calix[4]arenes **3a** (a), **4a** (b), **5a** (c), and **6a** (d).

involving the rotations of phenol rings. Monomethoxycalix[4]arene **3a** can interconvert to 1,2Alt or 1,3Alt with barriers not higher than 11.4 and 15.2 kcal mol⁻¹, respectively. The 0000~AA of 1,2-dimethoxycalix[4]arene **4a** can interconvert to 0011~AA passing barriers of only 11.7 and 12.1 kcal mol⁻¹, respectively. The interconversion of the global minimum 0000~AA of **4a** to one of the 0100/1000 stable Paco conformers involves an anisole ring rotation. The minimum barrier for this conversion is 29.2 kcal mol⁻¹ for 0000~BA \rightarrow 1000~AA. The 1000 and 0100 Paco conformers can interconvert by reversal of hydrogen bonding direction, a process that is assumed to proceed via a low free energy barrier,²⁹ or by low barrier rotation of the two phenol rings where, for instance, the 1000 conformer interconverts into the 1011 conformer (which is the inverted 0100 conformer). The Cone of 1,3-dimethoxy derivative **5a** can interconvert with low barriers to Paco and 1,3Alt conformers. Finally, the stable Cone conformers of trimethoxycalix[4]arene **6a** can interconvert to Paco with a barrier of 10.2 kcal mol⁻¹, and the stable Paco conformers can interconvert with comparable barriers to 1,2Alt or 1,3Alt conformers. However,

the interconversion of the most stable Cone 0000~AAA to one of the stable Paco conformers involves an anisole ring rotation with a minimum barrier of 27.0 kcal mol⁻¹ (0000~ABA \rightarrow 0100~AAA). The coalescence of NMR signals, observed¹⁰ for some partially methylated calix[4]arenes can involve low barrier rotations of phenol rings. The question remains how the stable Cone and Paco conformers of **4a** and **6a** interconvert. The calculated barriers for these interconversions are comparable to the barriers of the Cone \rightarrow Cone' interconversions, which were considered too large to allow interconversions at room temperature. In the calculations, no solvents effects were considered. At least for *p*-*tert*-butyl-tetramethoxycalix[4]arenes, the Paco \rightarrow 1,2Alt barrier is strongly influenced by the solvent.³⁰ Furthermore, the barriers of tetrahydroxycalix[4]arenes **1** can be lowered by the solvent, especially when it can act as a hydrogen-bond acceptor.³¹

Conclusions

The conformational distributions and Cone \rightarrow Cone' pathways have been successfully calculated for partially methylated calix[4]arenes **3a–6a**. The conformational distributions are generally in accordance with NMR data obtained for the *p*-*tert*-butyl derivatives **3b–6b**. Only for trimethoxycalix[4]arene **3a** was the calculated main conformer not Cone but Paco. The unidentified minor conformations found by NMR are most probably Paco conformers where one methoxy-bearing ring has rotated. The order of the calculated barriers for the Cone \rightarrow Cone' interconversions is monomethoxy- (35.1 kcal mol⁻¹) > 1,2-dimethoxy- (32.2 kcal mol⁻¹) \approx 1,3-dimethoxy- (30.3 kcal mol⁻¹) > trimethoxycalix[4]arene (27.0 kcal mol⁻¹), as was predicted qualitatively. All interconversion pathways proceeded via the 1,3Alt, although the pathways via the 1,2Alt are only slightly higher in energy. The rate-limiting step involved in all cases the rotation of a methoxy-bearing ring. The high inversion barriers of Cone \rightarrow Cone' interconversion are caused by the cooperative barriers of hydrogen bonds rupture and the steric barrier of rotating a methoxy group through the annulus. This cooperative effect is so strong that the Cone \rightarrow Cone' conversion is blocked at room temperature. Other conformational interconversions involving rotations of phenols ring have lower free energy barriers.

Supporting Information Available: Tables 3S–10S giving results of all calculations of conformational distributions and transition states of partially methylated calix[4]arenes **3a–6a** (total of 12 pages). Ordering information is given on any current masthead page.

References and Notes

- (1) (a) Gutsche, C. D. *Calixarenes*; Royal Society of Chemistry: Cambridge, 1989; (b) *Calixarenes. A versatile Class of Compounds*; Vicens, J.; Böhrer, V. Eds.; Kluwer Academic: Dordrecht, 1991; (c) Böhrer, V. *Angew. Chem., Int. Ed. Engl.* **1995**, *34*, 717; (d) Ikeda, A.; Shinkai, S. *Chem. Rev.* **1997**, *97*, 1713.
- (2) (a) Gutsche, C. D.; Reddy, P. A.; *J. Org. Chem.* **1991**, *56*, 4783; (b) Iwamoto, K.; Araki, K.; Shinkai, S. *J. Org. Chem.* **1991**, *56*, 4955; (c) Verboom, W.; Datta, S.; Asfari, Z.; Harkema, S.; Reinhoudt, D. N. *J. Org. Chem.* **1992**, *57*, 5394.
- (3) Iwamoto, K.; Araki, K.; Shinkai, S. *J. Org. Chem.* **1991**, *56*, 4955.
- (4) Gutsche, C. D.; Dhawan, B.; Levine, J. A.; No, K. H.; Bauer, L. J. *Tetrahedron* **1983**, *39*, 409.
- (5) Groenen, L. C.; van Loon, J.-D.; Verboom, W.; Harkema, S.; Casnati, A.; Ungaro, R.; Pochini, A.; Ugozzoli, F.; Reinhoudt, D. N. *J. Am. Chem. Soc.* **1991**, *113*, 2385.
- (6) The ethyl and acetoxy substituents can pass through the calix[4]arene cavity at higher temperatures (>100 °C for ethyl and >150 °C for acetoxy).

- (7) Akabori, S.; Sannohe, H.; Habata, Y.; Mukoyama, Y.; Ishii, T. *J. Chem. Soc., Chem. Commun.* **1996**, 1467.
- (8) Stewart, D. R.; Krawiec, M.; Kashyap, R. P.; Watson, W. H.; Gutsche, C. D. *J. Am. Chem. Soc.* **1995**, *117*, 586.
- (9) Alfieri, C.; Dradi, E.; Pochini, A.; Ungaro, R. *Gazz. Chim. Ital.* **1989**, *119*, 335.
- (10) Groenen, L. C.; Steinwender, E.; Lutz, B. T. G.; van der Maas, J. H.; Reinhoudt, D. N. *J. Chem. Soc., Perkin Trans. 2* **1992**, 1893.
- (11) Iwamoto, K.; Araki, K.; Shinkai, S. *Tetrahedron* **1991**, *47*, 4325.
- (12) Grootenhuis, P. D. J.; Kollman, P. A.; Groenen, L. C.; Reinhoudt, D. N.; van Hummel, G. J.; Uguzzoli, F.; Andreetti, G. D. *J. Am. Chem. Soc.* **1990**, *112*, 4165.
- (13) Fischer, S.; Grootenhuis, P. D. J.; Groenen, L. C.; van Hoorn, W. P.; van Veggel, F. C. J. M.; Reinhoudt, D. N.; Karplus, M. *J. Am. Chem. Soc.* **1995**, *117*, 1611.
- (14) See, for instance, the crystal structures of the Cones of 1,3-dimethoxycalix[4]arenes **5a** and **5b**, trimethoxycalix[4]arene **6b**, and 1,2-diethoxycalix[4]arene, or the energy-minimized Paco or 1,2Alt conformations of the tetrahydroxycalix[4]arene in ref 13.
- (15) Kanters, J. A.; Schouten, A.; Steinwender, E.; van der Maas, J. H.; Groenen, L. C.; Reinhoudt, D. N. *J. Mol. Struct.* **1992**, *269*, 49.
- (16) Brooks, B. R.; Bruccoleri, R. E.; Olafson, B. D.; States, D. J.; Swaminathan, S.; Karplus, M. *J. Comput. Chem.* **1983**, *4*, 187.
- (17) Brooks, B. R.; Janežič, D.; Karplus, M. *J. Comput. Chem.* **1995**, *12*, 1522.
- (18) Hill, T. L. *An Introduction to Statistical Thermodynamics*; Addison-Wesley Publishing: Reading, 1960.
- (19) van Hoorn, W. P.; Briels, W. J.; van Duynhoven, J. P. M.; van Veggel, F. C. J. M.; Reinhoudt, D. N. *J. Org. Chem.*, accepted.
- (20) Fischer, S.; Karplus, M. *Chem. Phys. Lett.* **1992**, *194*, 252.
- (21) (a) Fischer, S.; Michnick, S.; Karplus, M. *Biochemistry*, **1993**, *32*, 13830; (b) Fischer, S.; Dunbrack, R. L., Jr.; Karplus, M. *J. Am. Chem. Soc.* **1994**, *116*, 11931; (c) Verma, C. S.; Fischer, S.; Caves, L. S. D.; Roberts, G. C. K.; Hubbard, R. E. *J. Phys. Chem.* **1996**, *100*, 2510.
- (22) van Hoorn, W. P.; van Veggel, F. C. J. M.; Reinhoudt, D. N. *J. Org. Chem.* **1996**, *61*, 7180.
- (23) Note that all Cone \rightarrow Paco \rightarrow 1, 2Alt/1, 3Alt steps do have an equivalent 1, 2Alt/1, 3Alt \rightarrow Paco' \rightarrow Cone' step, but that these are not simple mirror images.
- (24) Morshuis, M. G. H. *Program written in C*, available on request.
- (25) A perfect Cone is a C_{4v} symmetric Cone (without taking into account the methoxy group that makes the monomethoxycalix[4]arene completely asymmetric).
- (26) (a) Harada, T.; Rudzinski, J. M.; Ōsawa, E.; Shinkai, S. *J. Chem. Soc., Perkin Trans. 2*, **1992**, 2109; (b) Harada, T.; Rudzinski, J. M.; Ōsawa, E.; Shinkai, S. *Tetrahedron* **1993**, *49*, 5941.
- (27) Iwamoto, K.; Ikeda, A.; Araki, K.; Harada, T.; Shinkai, S. *Tetrahedron* **1993**, *49*, 9937.
- (28) In both 1,2-dimethoxy- and 1,3-dimethoxycalix[4]arene, two hydrogen bonds are formed, but OH is a better acceptor than OMe, making the hydrogen bonds in 1,2-dimethoxycalix[4]arene more favorable.
- (29) (a) Kim, Y.; *J. Am. Chem. Soc.* **1996**, *118*, 1522; (b) Brzezinski, B.; Urjasz, H.; Zundel, G. *J. Phys. Chem.* **1996**, *100*, 9021.
- (30) Blixt, J.; Detellier, C. *J. Am. Chem. Soc.* **1994**, *116*, 11957.
- (31) Gutsche, C. D.; Bauer, L. J. *J. Am. Chem. Soc.* **1985**, *107*, 6052.